

# Static properties of the dissipative random quantum Ising ferromagnetic chain

L. F. Cugliandolo,<sup>1,2</sup> G. S. Lozano<sup>3</sup> and H. Lozza<sup>3</sup>

<sup>1</sup> *Laboratoire de Physique Théorique et Hautes Énergies, Jussieu,*

*4 Place Jussieu, 75252 Paris Cedex 05, France*

<sup>2</sup> *Laboratoire de Physique Théorique, École Normale Supérieure de Paris,*

*24 rue Lhomond, 75231 Paris Cedex 05, France,*

<sup>3</sup> *Departamento de Física, Universidad de Buenos Aires,*

*Pab. I, Ciudad Universitaria 1428, Argentina.*

September 20, 2018

## Abstract

We study the zero temperature static properties of dissipative ensembles of quantum Ising spins arranged on periodic one dimensional finite clusters and on an infinite chain. The spins interact ferro-magnetically with nearest-neighbour pure and random couplings. They are subject to a transverse field and coupled to an Ohmic bath of quantum harmonic oscillators. We analyze the coupled system using Monte Carlo simulations of the classical two-dimensional counterpart model. The coupling to the bath enhances the extent of the ordered phase, as found in mean-field spin-glasses. In the case of finite clusters we show that a generalization of the Caldeira-Leggett localization transition exists. In the case of the infinite random chain we study the effect of dissipation on the transition and the Griffiths phase.

KEYWORDS: Spin chain, disorder, dissipation, Monte Carlo

# 1 Introduction

The influence of quenched disorder [1, 2] on the one hand and the effect of the coupling to an environment [3, 4], on the other, on *finite* dimensional quantum spin models have been separately analyzed recently. The former introduce Griffiths-Mc Coy singularities that are particularly important for quantum systems [1, 5, 6]. Dissipation implies decoherence and the coupling to a quantum bath generates highly non-trivial localization phenomena at least for a single two-level system [7]. The combined effect of quenched disorder and the coupling to a quantum reservoir has only been analyzed in mean-field models so far [8, 9].

A ring of quantum Ising spins is probably the simplest finite dimensional model exhibiting a phase transition from a paramagnetic (PM) to a ferromagnetic (FM) phase where one can analyze the mixed effect of disorder and dissipation. Indeed, the bath introduces long-range ferromagnetic interactions in the imaginary-time direction that add to the nearest-neighbor ferromagnetic couplings due the quantum nature of the spins and, at zero temperature, one finds a phase transition even for finite size clusters. The  $d + 1$  equivalent classical problem is characterized by perfect correlation in the imaginary-time direction and the effect of disorder is consequently very strong. For sufficiently large system sizes and, in particular, in the thermodynamic limit rare regions in the sample may have a very strong effects on the properties close to the phase transition, giving rise to very interesting Griffiths phenomena.

The zero-temperature critical behavior of the isolated finite dimensional infinite system in one, two and three dimensions has been studied in detail in a series of analytic [1, 10, 11] and numerical papers [12, 13, 14, 15, 16, 17]. An ‘infinite randomness fixed point scenario’, in which the system appears more and more random at larger and larger scales, emerged [1]. The critical behavior is quite uncommon, with activated scaling on the transition and very large distributions of local properties in a finite interval close to the quantum critical point that lead to different typical and average values and the divergence of the global susceptibility well within the paramagnetic phase.

In this paper we investigate the effect of Ohmic dissipation on the equilibrium properties of small clusters and an infinite chain of quantum Ising spins with ferromagnetic exchange interactions of pure and random type. We focus on the following questions: (i) How is the Caldeira-Leggett localization transition modified when several ferro-magnetically interacting spins are coupled to an environment. (ii) Which are the characteristics of the quantum phase transition, as a function of the transverse field and the coupling strength to the bath, for finite clusters and in the thermodynamic limit. (iii)

Whether the peculiar phenomenology of the isolated random Ising chain [1], especially in its paramagnetic phase, also exists when it is coupled to an environment. Conflicting predictions, based on phenomenological droplet-like arguments [18] and the analysis of some simplified models [19], appeared in the literature recently. We address these questions here using Monte Carlo simulations of the equivalent classical model in  $d = 2$  with short-range interaction in the spatial direction and long-range interactions in the imaginary-time direction as introduced by the coupling to the bath.

The paper is organized as follows. In Sect. 2 we define the model. Section 3 is devoted to a brief description of the Monte Carlo method used to generate the numerical data. We also summarize in this Section the parameters studied. In Sect. 4 we explain our results. Finally, in Sect. 5 we present our conclusions and discuss some areas of applicability of our results.

## 2 The model

The Hamiltonian of the random quantum Ising spin chain is

$$H_J = - \sum_{i=1}^N J_i \hat{\sigma}_i^z \hat{\sigma}_{i+1}^z - \sum_{i=1}^N \Gamma_i \hat{\sigma}_i^x - \sum_{i=1}^N h_i \hat{\sigma}_i^z. \quad (1)$$

The spins lie on the vertices of a periodic one dimensional lattice with  $N$  sites. They are represented by Pauli matrices satisfying the SU(2) algebra:  $[\hat{\sigma}_i^a, \hat{\sigma}_j^b] = \delta_{ij} \epsilon_{abc} i \hat{\sigma}_i^c$  with  $a, b, c = 1, 2, 3$  associated to  $x, y, z$ , respectively and  $i = 1, \dots, N$ . We consider  $J_i$ , the strength of the exchange interactions between nearest-neighbors, as independent quenched random variables in the interval  $0 < J_i < 1$  with uniform probability density. Without loss of generality, we choose  $J_i$  positive since for one dimensional lattices the sign of the interactions can be gauged away (even when the system is linearly coupled to the coordinates of the harmonic oscillators representing the bath). The next-to-last term is a coupling to a local transverse field that, for simplicity, we choose to be the same on all sites,  $\Gamma_i = \Gamma$ . The last term is a coupling to a longitudinal field that one may include to compute local susceptibilities.

The chain plus environment is modeled by

$$\hat{H} = \hat{H}_J + \hat{H}_B + \hat{H}_I + \hat{H}_{CT} \quad (2)$$

where  $\hat{H}_B$  is the Hamiltonian of the bath,  $H_I$  represents the interaction between the chain and the bath and  $H_{CT}$  is a counter-term that serves to eliminate an undesired mass renormalization induced by the coupling [20]. We assume that each spin in the system is coupled to its own set of  $N/N$

independent harmonic oscillators with  $\tilde{N}$  the total number of them. The bosonic Hamiltonian for the isolated reservoir is

$$\hat{H}_B = \sum_{l=1}^{\tilde{N}} \frac{1}{2m_l} \hat{p}_l^2 + \sum_{l=1}^{\tilde{N}} \frac{m_l \omega_l^2}{2} \hat{x}_l^2. \quad (3)$$

The coordinates  $\hat{x}_l$  and the momenta  $\hat{p}_l$  satisfy canonical commutation relations. For simplicity we consider a bilinear coupling,

$$\hat{H}_I = - \sum_{i=1}^N \hat{\sigma}_i^z \sum_{l=1}^{\tilde{N}} c_{il} \hat{x}_l, \quad (4)$$

that involves only the oscillator coordinates. The counter term reads

$$\hat{H}_{CT} = \sum_{l=1}^{\tilde{N}} \frac{1}{2m_l \omega_l^2} \left( \sum_{i=1}^N c_{il} \hat{\sigma}_i^z \right)^2. \quad (5)$$

The partition function of the whole system for a particular realization of the random exchange interactions is  $Z_J = \text{Tr} e^{-\beta \hat{H}}$ , involving a sum over all states of the chain and the bath. This problem can be mapped onto a classical model by using the Trotter-Suzuki formalism that amounts to writing the path-integral for the partition function as a sum over spin and oscillator variables evaluated on a discrete imaginary-time grid,  $\tau_t = t \Delta\tau$  with  $\Delta\tau \equiv \beta \hbar / N_\tau$ , labeled by the index  $t = 0, \dots, N_\tau - 1$ . We assume periodic boundary conditions in all directions with  $\beta \hbar$  the length in the  $\tau$  direction. This mapping is exact in the limit  $N_\tau \rightarrow \infty$ . In what follows, we use units such that  $k_B = \hbar = 1$ .

The integration over the bath variables can be performed explicitly; for an Ohmic bath the resulting classical action reads

$$\begin{aligned} \mathcal{A}[K_i, B, \alpha; s_i^t] = & - \sum_{t=0}^{N_\tau-1} \sum_{i=1}^N K_i s_i^t s_{i+1}^t - B \sum_{t=0}^{N_\tau-1} \sum_{i=1}^N s_i^t s_i^{t+1} \\ & - \frac{\alpha}{2} \sum_{t < t'}^{N_\tau-1} \sum_{i=1}^N \left( \frac{\pi}{N_\tau} \right)^2 \frac{s_i^t s_i^{t'}}{\sin^2(\pi |t - t'| / N_\tau)}, \end{aligned} \quad (6)$$

where we set  $h_i = 0$  and we dropped an irrelevant constant factor.  $s_i^t$  are  $N \times N_\tau$  classical Ising variables,  $s_i^t = \pm 1$ , representing the  $z$  component of the quantum spin at each instant  $\tau_t$  at site  $i$ . Notice that the bath is responsible for the appearance of long range ferromagnetic interactions in the  $\tau$  direction controlled by the chain-bath coupling parameter  $\alpha$ . From the

quantum nature of the spins, a nearest-neighbour ferromagnetic coupling also arises in the  $\tau$  direction. Its strength  $B$  is defined by

$$\exp -2B = \tanh(\Delta\tau\Gamma) , \quad (7)$$

and describes the intensity of the quantum fluctuations. Further, since  $J_i$  are quenched random variables, the random values of the spatial interactions

$$K_i = \Delta\tau J_i \quad (8)$$

are the same along each imaginary-time direction, *i.e.* depend only on the spatial label  $i$ .

### 3 Monte Carlo simulations

We analyze the static properties of the system by means of Monte Carlo simulations applied to the effective (1 + 1) dimensional partition function,

$$Z_J = \sum_{s_i^t = \pm 1} e^{-\mathcal{A}[K_i, B, \alpha; s_i^t]} . \quad (9)$$

The sum over all spin configurations accounts for the statistical average that we denote, henceforth, with angular brackets. In the disordered cases, the thermodynamic properties and, in particular, the phase transition follow from the analysis of the free-energy density averaged over the probability distribution of the random exchanges. We indicate this average with square brackets.

Taking advantage of the fact that the ferromagnetic models are not frustrated (all  $J_i > 0$ ), we use an efficient Monte Carlo algorithm that adapts the cluster updates [21] to the case with long range ferromagnetic interactions [22]. In addition, in order to avoid running several simulations with similar parameters, we use histogram methods to scan the space of parameters near a phase transition [23].

The classical counterpart model is defined on a rectangular lattice with size  $N \times N_\tau$ . The zero temperature limit,  $\beta \rightarrow \infty$ , is achieved by taking the thermodynamic limit in the imaginary time direction,  $N_\tau \rightarrow \infty$ . We used various system sizes varying the aspect ratio of the  $2d$  sample. We took  $N$  from 1 to 32 and  $N_\tau$  from 4 to 1024. We found that up to 400 Monte Carlo sweeps were needed to equilibrate the largest sample sizes (note the efficiency of the cluster algorithm!). We simulated up to 2048 different realizations of the exchange interactions to account for the effect of disorder.

We concentrate on the critical properties of finite and infinite periodic chains at zero temperature. As we have already set the disorder scale  $0 <$

$J_i < 1$ , a complete description of the state of the system is given by the dimensionless parameters  $\alpha$  and  $\Delta\tau\Gamma$ . For comparison, we also simulate the non-random chain coupled to an Ohmic bath replacing the random variables  $J_i$  with uniform distribution between 0 and 1 by a constant value equal to the maximum,  $J_i = 1$ .

## 4 Results

In this Section we present the results of our numerical simulations.

As mentioned before, we used system sizes ranging from  $N = 1$  to  $N = 32$ . We separate our results in two groups, small  $N$  ( $N \leq 4$ ), and large  $N$  ( $N > 4$ ). In the first group we intend to study whether the random exchange interactions modify the physics of the well known Caldeira-Leggett model while for the second group our results generalize those reported in [3] (where no random interactions are present) and those reported in [1, 14, 15, 24] (where no bath is present).

### 4.1 Phase diagram

#### 4.1.1 Analysis of the Binder parameter

The phase transition in the  $(\Delta\tau\Gamma, \alpha)$ -plane can be found by analyzing the Binder ratio

$$g_{av} \equiv \frac{1}{2} \left[ 3 - \frac{\langle m^4 \rangle}{\langle m^2 \rangle^2} \right], \quad (10)$$

where the angular brackets indicate the statistical average and the square brackets denote the average over disorder (if there is no disorder, this step is not necessary). The magnetization density is defined as

$$m \equiv \frac{1}{NN_\tau} \sum_{i=1}^N \sum_{t=0}^{N_\tau-1} s_i^t. \quad (11)$$

The analysis of the Binder ratio presents different aspects whether we consider a finite cluster or its thermodynamic limit.

#### (i) Small $N$

When  $N$  is finite the zero-temperature limit of the quantum problem corresponds to a classical model defined on a stripe of finite width ( $N < \infty$ ) and infinite height ( $N_\tau \rightarrow \infty$ ). In this case, the usual finite size scaling analysis of the adimensional Binder parameter can be applied. The critical values are easily found by plotting  $g_{av}$  as a function of  $\alpha$  for several values

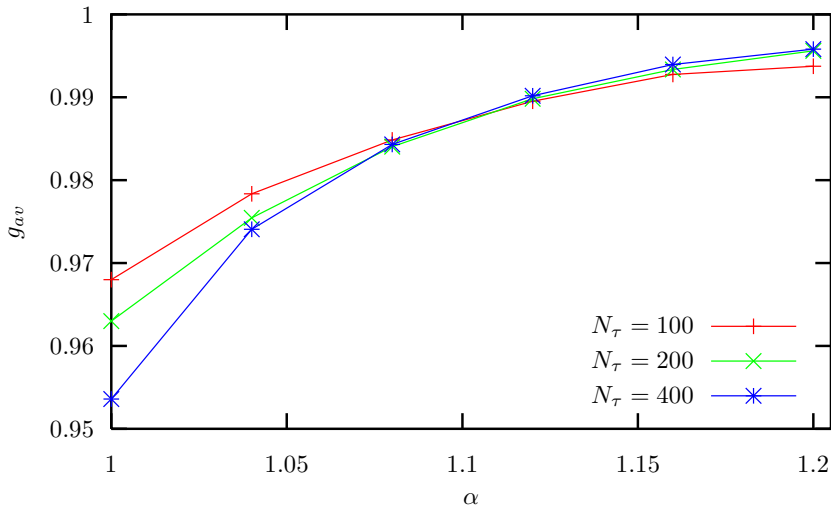


Figure 1: (Color on-line.) The Binder cumulant as a function of  $\alpha$  for  $N = 1$  with  $\Delta\tau_c\Gamma_c = 0.48$ . The localization transition occurs at  $\alpha_c = 1.10 \pm 0.02$ .

of  $N_\tau$ . The dimensionless combination of momenta in Eq. (10) yields  $g_{av}$  independent of size at criticality. Then,  $\alpha_c$  can be located by finding the intersection of the  $g_{av}$  curves against  $\alpha$  for several  $N_\tau$  [25] for every choice of  $\Delta\tau_c\Gamma_c$ .

The case  $N = 1$  corresponds to the well known problem of a two level system coupled to a bath. In this case we expect a transition from an incoherent state to a localized one at  $\alpha_c = 1.0$  as analytically demonstrated by Leggett *et al.* [7]. As a test for our numerical algorithm, we re-derive this result numerically. In Fig. 1 we show an example with  $N = 1$  and  $\Delta\tau_c\Gamma_c = 0.48$ , where we see that the curves cross at  $\alpha_c = 1.10 \pm 0.02$  (the error measures the precision on the crossing point). We build the phase diagram by repeating these steps for several values of  $\Delta\tau_c\Gamma_c$ .

We use the same method to obtain the critical line for  $N = 2$  and 4 both for random and non-random exchange interactions. In Fig. 2 we show the phase diagram for  $N = 1, 2, 4$ . In general, it is hard to determine  $\alpha_c$  for  $\Delta\tau\Gamma < 0.2$  where  $g_{av}$  varies less than 0.1% and  $\alpha_c$  is masked by the noise.

For  $N = 1$  the critical values  $(\Delta\tau_c\Gamma_c, \alpha_c)$  are well fitted by a linear function that for  $\Delta\tau_c\Gamma_c \rightarrow 0$  approaches the analytical result  $\alpha_c = 1$  [7]. The localization transition moves to lower values of  $\alpha_c$  when  $N$  increases. In addition, for finite  $N$ , the disordered chain has a lower  $\Delta\tau_c\Gamma_c$  for a given  $\alpha_c$ . However, this difference tends to reduce when  $\Delta\tau_c\Gamma_c \rightarrow 0$ .

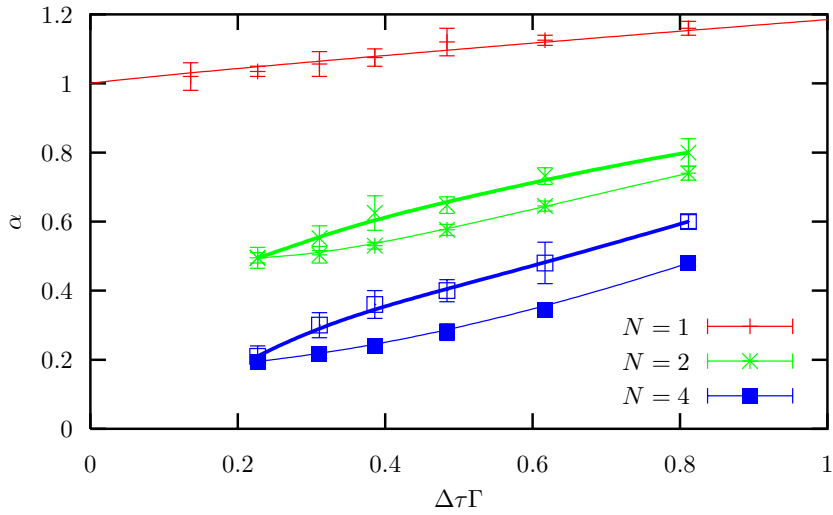


Figure 2: (Color on-line.) Critical boundary  $(\Delta\tau_c\Gamma_c, \alpha_c)$  for small clusters,  $N \leq 4$ . For  $N = 1$  this corresponds to the localization transition in the Caldeira-Leggett model. The data are well fitted by a linear function reaching  $\alpha_c = 1$  at  $\Delta\tau_c\Gamma_c = 0$ . For  $N > 1$ , we show the transition curve for systems with random exchange interactions (thick lines) and non-random exchange interactions (thin lines).

(ii) Thermodynamic limit

In the thermodynamic limit the finite size scaling analysis must be done using the parameters  $N$  and  $N_\tau$  and, naively, one is forced to assume a scaling relation between them. The Binder cumulant is an adimensional quantity that on the phase transition must scale as

$$g_{av} \sim \tilde{g}(N/\xi, y) \quad (12)$$

where  $\xi$  is the spatial correlation length,  $\tilde{g}$  is a scaling function and  $y$  is a ratio between the imaginary-time size  $N_\tau$  and some adequate function of the spatial size  $N$ . For instance, one has

$$y = \begin{cases} N_\tau/N^z & \text{conventional scaling ,} \\ N_\tau/e^{N\bar{z}} & \text{activated scaling .} \end{cases} \quad (13)$$

A simple argument shows that for fixed  $N$  and generic values of the other parameters the Binder cumulant attains a maximum as a function of  $N_\tau$  [12, 13]. This argument still holds when long-range interaction are introduced by the bath. Indeed, when  $N_\tau$  is very small with respect to  $N$ , one effectively



has a very long one-dimensional stripe (along the spatial dimension) and the long-range interactions induced by the bath on the imaginary-time direction are irrelevant. Moreover, for the values of the parameters that are close to the phase transition of the infinite  $2d$  system, one is well above the transition of the one dimensional system and  $g_{av} \rightarrow 0$ . In the opposite limit of  $N_\tau \gg N$  one is back in the kind of finite cluster problem discussed in the previous paragraphs. Now, for the parameters chosen, the new one-dimensional model should have a finite correlation length away from its critical line and  $g_{av} \rightarrow 0$  as well. For  $N$  and all other parameters fixed  $g_{av}$  should then reach a maximum as a function of  $N_\tau$ . The maximum value  $g_{av}^{max}$  is independent of  $N$  at criticality, see Fig. 3. We extrapolate the thermodynamic critical values by considering a collection of chains with sizes ranging from  $N = 8$  to  $N = 32$ . For each  $\Delta\tau_c\Gamma_c$  we looked for the value of  $\alpha$  such that the  $N$ -independent maximum is reached. The phase diagram in Fig. 4 has been built repeating these steps. The error-bars estimate the dispersion on the values of  $g_{av}$  arising from the Monte Carlo method and the disordered interactions after performing error propagation on Eq. (10).

In Fig 4 we see that the infinite chain has a phase transition even at  $\alpha = 0$ , in contrast to the small  $N$  case. We find that the phase transition curve may be accurately described by a power law, and the size of the ordered phase increases with increasing coupling to the environment. For comparison we also show the transition line for a non-random Ising chain with Ohmic dissipation [3] as determined by using the same procedure and similar sizes as the ones we use in the disordered problem.

The critical values for  $\Delta\tau_c\Gamma_c$  with  $\alpha_c = 0$ , which corresponds to switching off the bath, agree with well established analytical results for both the random and non-random cases [5, 26]. Indeed, the critical values of the random and non-random models in terms of our variables are  $\Delta\tau_c\Gamma_c = 0.25$  and  $\Delta\tau_c\Gamma_c = 0.44$  respectively, which agree with our numerical calculations [27].

#### 4.1.2 The global linear susceptibility

In a usual paramagnetic to ferromagnetic phase transition one can expect to identify the critical line by looking for the location of the divergence of the global linear susceptibility defined as

$$\chi \equiv \sum_{i=1}^N \chi_i = \sum_{i=1}^N \left[ \frac{\partial \langle m_i \rangle}{\partial h_i} \Big|_{h_i=0} \right] = \frac{1}{N_\tau} \sum_{i=1}^N \left[ \langle m_i^2 \rangle - \langle m_i \rangle^2 \right], \quad (14)$$

and

$$m_i = \sum_{t=1}^{N_\tau} s_i^t. \quad (15)$$

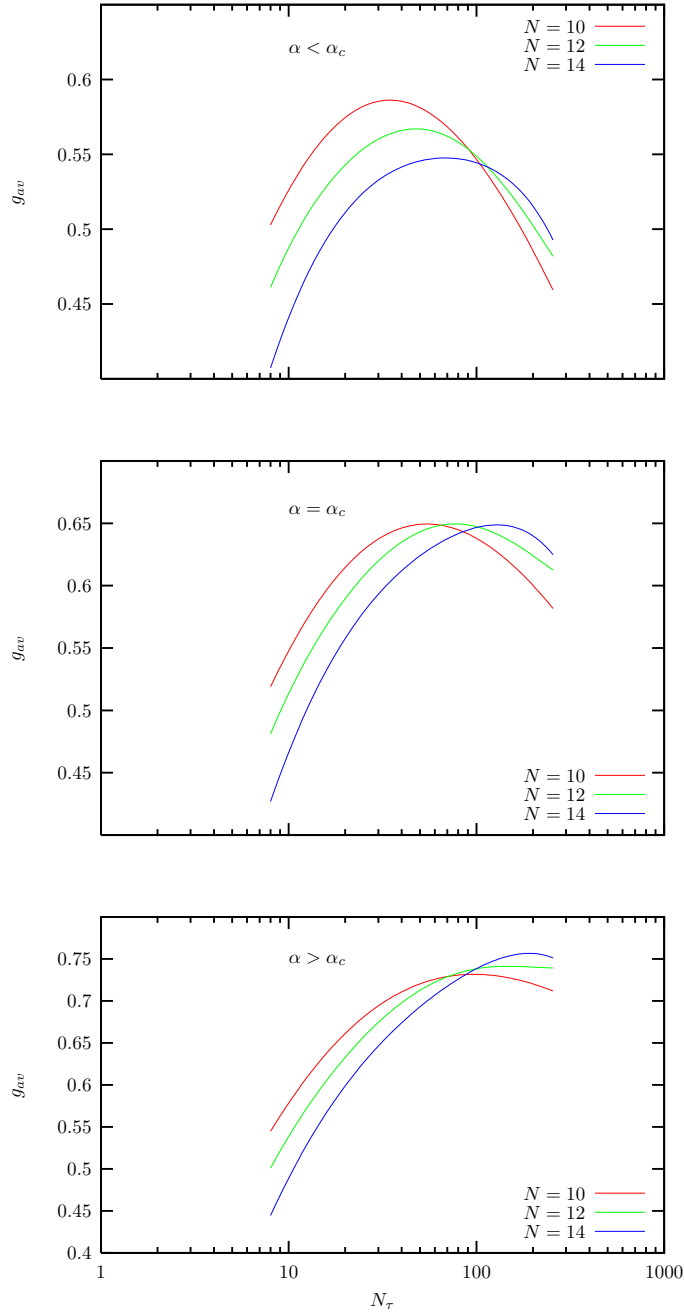


Figure 3: (Color on-line.) Typical behavior of the Binder cumulant at fixed  $\Delta\tau_c\Gamma_c$  and in a neighborhood of its corresponding  $\alpha_c$ . The maximum of  $g_{av}$  is independent of  $N$  only at  $\alpha = \alpha_c$ , see the central panel.

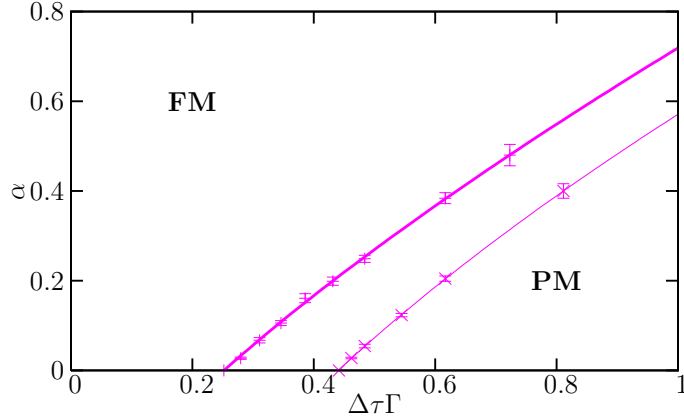


Figure 4: (Color on-line.) Phase diagram for  $N = \infty$ . We show this line for the disordered chain with a uniform distribution of exchanges on the interval  $[0, 1]$  (thick lines) and the non-random chain with  $J = 1$  (thin lines).

With the aim of later studying the effect of dissipation on the distribution of local susceptibility of the random chain, we attempted to analyze the divergence of the global susceptibility in finite clusters [28]. Indeed, when  $N < \infty$  we expect to find a divergence of  $\chi$  only on the phase transition, and not within the paramagnetic phase as found for the isolated random infinite chain [1]. For finite values of the number of imaginary-time slices  $N_\tau$  we found that the global linear susceptibility at  $\alpha$  fixed has a peak at value of  $\Delta\tau\Gamma$  that is quite higher than the one obtained from the analysis of the Binder parameter in the limit  $N_\tau \rightarrow \infty$ . As expected the height of the peak increases while its position moves towards lower values of  $\Delta\tau\Gamma$  when  $N_\tau$  increases. For  $N = 4$ ,  $N_\tau = 128$  and  $\alpha = 0.45$  we find a deviation of the order of 10%. This indicates that the finite size effects in  $N_\tau$  are still very important. Note that this holds for the ordered and disordered system as well. These observations are illustrated in Figs. 5.

In Fig. 6 we attempted to compare the form of the peak for similar ordered and disordered systems, *i.e.* with the same size and under the effect of the same external bath. We note that the peak is more pronounced in the ordered case and the deviation between its location at finite  $N_\tau$  and the asymptotic

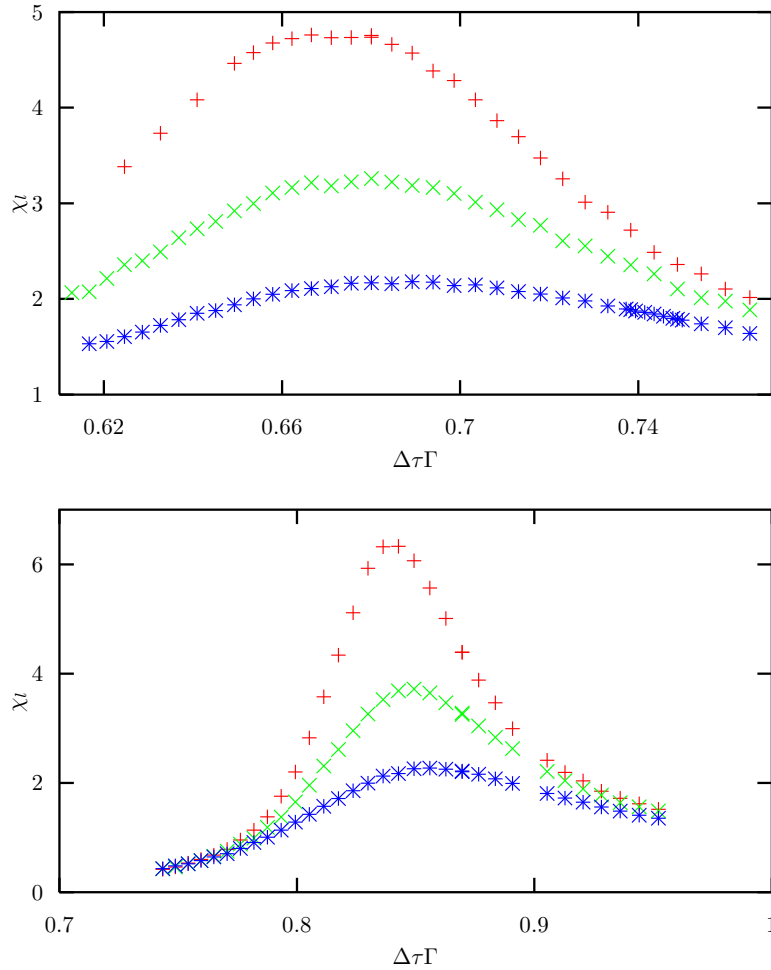


Figure 5: The average global linear susceptibility  $\chi$  for  $\alpha_c = 0.45$  as a function of  $\Delta\tau\Gamma$ .  $N = 4$  and  $N_\tau = 128, 64, 32$  from top to bottom. Top panel: Random interactions. Bottom panel: pure ferromagnet.

$N_\tau \rightarrow \infty$  one is less pronounced. More precisely, we found

$$(\Delta\tau\Gamma)_c = \begin{cases} \text{Binder} & \text{Peak in } \chi \\ N_\tau \rightarrow \infty & N_\tau = 128 \\ 0.77 & 0.84 & \text{ordered} \\ 0.55 & 0.66 & \text{disordered} \end{cases} \quad (16)$$

In conclusion, we found that the extrapolation of the finite  $N_\tau$  susceptibility data to the thermodynamic limit is indeed very hard [30]. A detailed analysis of the scaling behavior needs to be performed but it currently goes beyond our computational power. This failure has to be kept in mind when

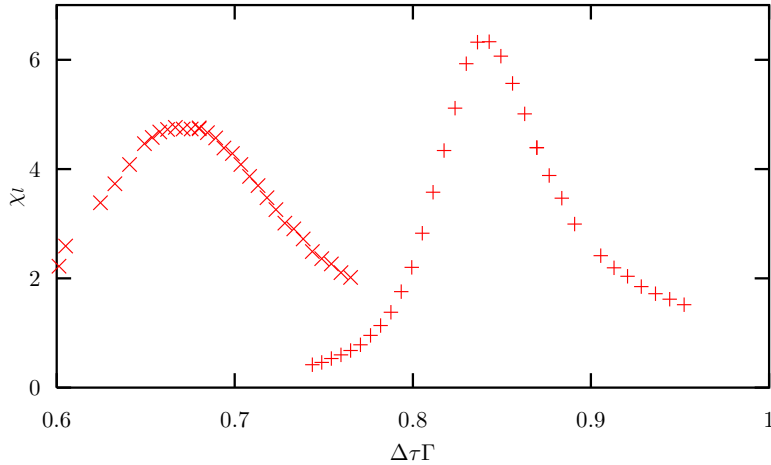


Figure 6: Comparison between the global linear susceptibility for the model with random (left) and pure (right) systems with  $N = 4$ ,  $N_\tau = 128$  and  $\alpha_c = 0.45$ .

trying to analyze the dynamic properties of the dissipative disordered Ising chain in the paramagnetic phase, see Sect. 4.2.

## 4.2 Critical scaling: conventional or activated?

One of peculiarities of the critical behavior of the isolated quantum Ising chain with random interactions is that the critical scaling is activated instead of conventional power law type. We wish to investigate whether a similar behavior persists when Ohmic dissipation is included.

### 4.2.1 The Binder ratio

The Binder ratio not only gives a criterion to find the phase transition curve but also helps to derive scaling laws. The study of the scaling laws for the function  $g_{av}$  can in principle provide an answer to the question of whether the critical behavior is of conventional or activated type. Finite size scaling implies that dimensionless quantities should scale as functions of  $N/\xi$ , and as either  $N_\tau/N^z$  in the case of conventional scaling or  $N_\tau/e^{N\bar{z}}$  in the case of activated scaling. At the critical point, the correlation length in the spatial direction,  $\xi$ , diverges. This suggests that the scaling variable should be  $N_\tau/N_\tau^{max}$  or  $\ln N_\tau/\ln N_\tau^{max}$  in each case respectively, where  $N_\tau^{max}$  is the value of  $N_\tau$  that maximizes  $g_{av}$  [13]. This way of analyzing the data has the advantage of not needing to determine the critical exponents  $z$  or  $\bar{z}$ .

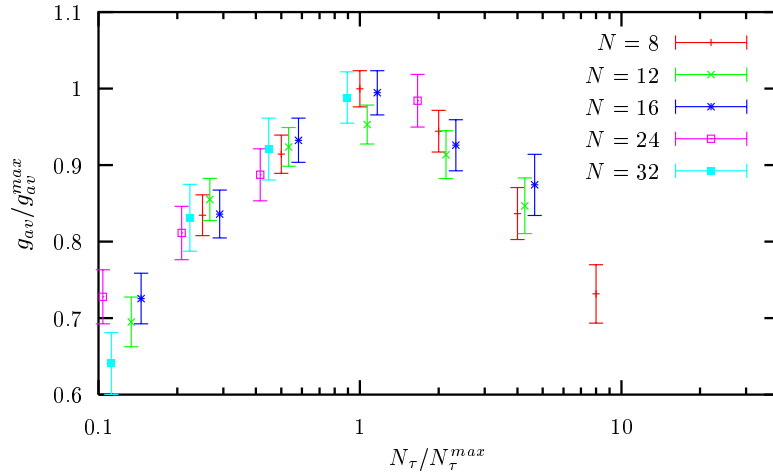


Figure 7: (Color on-line.) Test of conventional scalings at  $(\Delta\tau_c\Gamma_c = 0.48, \alpha_c = 0.25)$ .

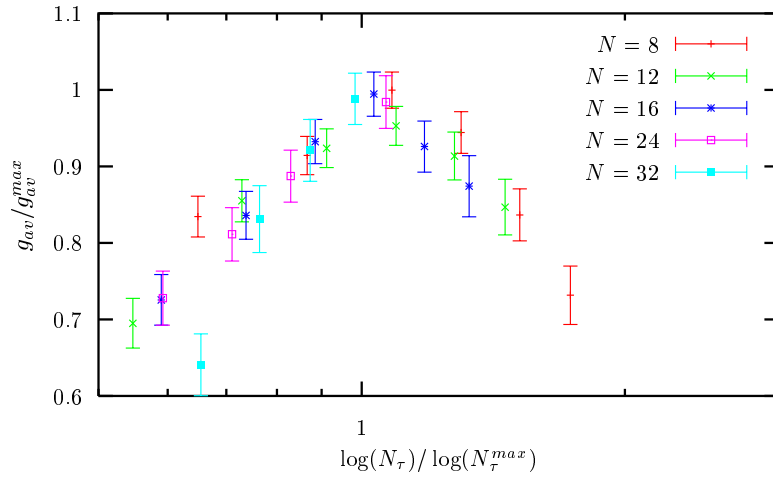


Figure 8: (Color on-line) Test of activated scalings at  $(\Delta\tau_c\Gamma_c = 0.48, \alpha_c = 0.25)$ .

However the interpretation of the numeric results is delicate. Even for  $\alpha = 0$ , where it is possible to show analytically the activated scaling [1], it has been hard to distinguish between both types of scaling by means of Monte Carlo simulations [12, 13, 24]. In particular, in  $d = 1$  the numerical data confirmed the analytic prediction only when a mapping to fermions was used [14].

In Fig 7 we show the scaling of the Binder parameter,  $g_{av}/g_{av}^{max}$ , with  $N/N_\tau^{max}$  (conventional) and in Fig 8 with  $\ln N/\ln N_\tau^{max}$  (activated). Both

scalings give almost the same critical values ( $\Delta\tau_c\Gamma_c, \alpha_c$ ) in agreement with our previous simpler analysis using the independence of the height of the maximum on  $N$  at criticality. Unfortunately, the two scaling plots are of quite similar quality and with the system sizes considered here we cannot distinguish between the two critical scalings.

#### 4.2.2 Distribution of local susceptibilities

An alternative analysis of the critical scaling in the disordered models is based on the study of the probability distribution function (pdf) of local linear and non-linear susceptibilities and how they behave when approaching the critical line.

In the isolated random chain the pdf of local linear and non-linear susceptibilities decay, for large values of the arguments, with a power law that decreases when approaching the quantum critical point. The inverse of this power is linked to the dynamic critical exponent and its divergence on the transition implies activated scaling. At a finite distance from the critical point the decay becomes sufficiently slow so as to lead to a divergent global susceptibility. One may wonder whether this phenomenon also occurs in the presence of dissipation.

To try to give an answer to this question we started by studying the pdf of local linear susceptibilities of finite clusters ( $N < \infty$ ). In Fig. 9 we show  $p(\ln \chi_i)$  for  $N = 4$  and four values of the number of imaginary-time slices,  $N_\tau = 32, 64, 128, 256$ , at  $\alpha = 0.45$  and  $\Delta\tau\Gamma = 0.66$ . A finite value of  $N_\tau$  gives a finite bound to the maximum possible  $\chi_i$ . This figure can be compared to the left-most curve in Fig. 20 in the first reference in [14] that has been obtained for  $N = 4$  and effectively with  $N_\tau \rightarrow \infty$ . This figure shows that the coupling to the external bath has not modified the form of the pdf in an important way.

Finally, we analyzed the decay of the probability density of the local linear susceptibilities when approaching the critical line. Each panel in Fig. 10 displays these pdfs for four values of  $\Delta\tau\Gamma$  and  $\alpha$  fixed. Each set of data, represented with different symbols, were obtained for different  $N$  and choosing  $N_\tau$  in such a way that the maximum in the Binder parameter is reached. The values of  $N$  are given in the captions. The straight lines are guides to the eye to indicate a possible power-law decay and the values of this power are given in the caption.

Even if it is clear from the figures that there is a trend to a decreasing power law decay as the transition is approached, a functional relation between this power and the distance to the critical line is hard to establish beyond doubt from the pure numerical data. Analytic guidance, as was necessary

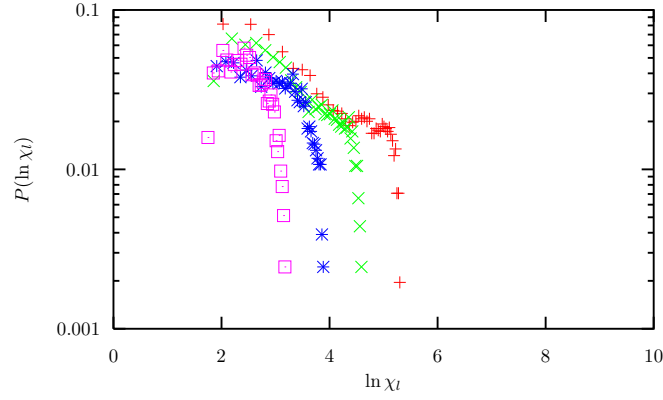


Figure 9: (Color on-line.) Probability distribution function of the local linear susceptibilities for a finite cluster with  $N = 4$  and (from left to right) four values of the number of imaginary-time slices,  $N_\tau = 32, 64, 128, 256$ .  $\alpha = 0.45$  and  $\Delta\tau\Gamma = 0.66$ .

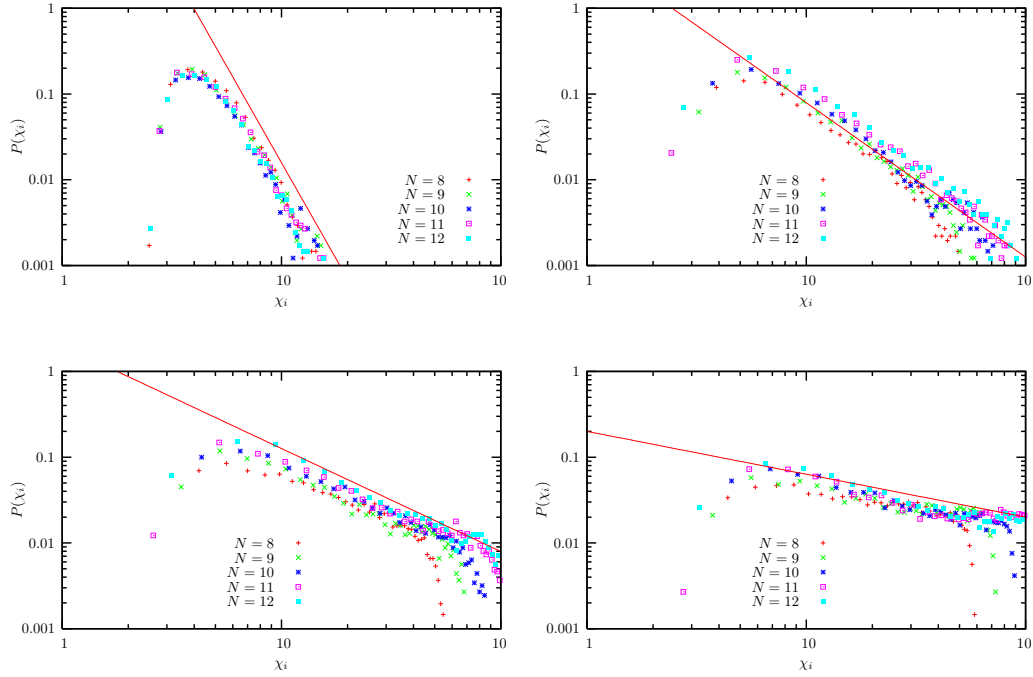


Figure 10: Probability distribution of the single site linear susceptibility.  $\Delta\tau\Gamma = 0.48$  (top left),  $0.43$  (top right),  $0.41$  (bottom left),  $0.39$  (bottom right).  $\alpha = 0.15$  in all cases. The slope of the straight lines indicated in each panel are  $b = 4.55$  (top left),  $1.82$  (top right),  $1.20$  (bottom left),  $0.5$  (bottom right).



to interpret correctly the numerical data for the isolated case, seems to be necessary here too.

## 5 Conclusions

With a careful analysis of the Monte Carlo data we succeeded in determining the phase boundary between the paramagnetic and ferromagnetic phases in finite and infinite rings of interacting quantum Ising spins in a transverse field and coupled to an external environment. While for finite number of spins there is no phase transition in the limit  $\alpha \rightarrow 0$ , in the thermodynamic limit one recovers the critical points of McCoy and Wu in the disordered case, and Onsager in the ordered problem.

The method that we used allowed us to determine the Caldeira-Leggett critical value  $\alpha_c = 1$  for  $N = 1$  with relatively little numerical effort. We used a similar analysis to find the phase transition of interacting finite clusters under the effect of an Ohmic bath. A similar analysis could be used to study the influence of other types of baths (sub-Ohmic, super-Ohmic) for which less analytical results are available.

The coupling to the bath enhances the extent of the ordered phase, as found in mean-field spin-glasses [8, 9] and in the ordered ferromagnetic Ising chain [3]. The Griffiths phase still exists as characterised by large distributions of the local linear and non-linear susceptibilities (the latter are not shown in the text). We expect to find similar results in higher finite dimensions and when frustration is included (*i.e.* when negative exchanges also exist).

Our results for the type of scaling characterizing the phase transition for the disordered and dissipative infinite chain are not conclusive. Even if we have no evidence for the failure of the activated scaling of the isolated case when dissipation is included, we cannot exclude this possibility from our numerical data. It is important to notice that the activated scaling in the dissipation-less problem was found analytically and it was very hard to confirm numerically. It would be extremely interesting to extend Fisher's renormalization group approach to the case of the random chain coupled to an environment to give a definitive answer to this question.

The systems we studied admit applications in a variety of fields. Quantum (spin) glass phases have been observed experimentally in several compounds [32]; the role played by the coupling to the environment in their low-temperature anomalous properties has not been fully elucidated yet. Interacting spin systems are now becoming popular as possible toy models for quantum computers, with the Ising spins representing the qubits. It is ob-

vously very important in this context to establish the effect of the coupling to the bath. Another motivation for our study comes from the proposal in [18] to describe non-Fermi liquid behavior in certain  $f$ -electron systems with a similar model (see also [19]). Finally, while classical phase transitions are well understood by now, the same does not apply to quantum phase transitions at zero temperature [6, 33]. For all these reason we believe that this (and related ones) are interesting problems that deserve further study.

Acknowledgements. LFC is a member of the Institut Universitaire de France and acknowledges financial support from an Ecos-Sud travel grant, the ACI project “Optimisation algorithms and quantum disordered systems” and the ICTP-Trieste, as well as hospitality from the Universidad de Buenos Aires and the Universidad Nacional de Mar del Plata, Argentina and ICTP-Trieste where part of this work was prepared. This research was supported in part by SECYT PICS 03-11609 and PICS 03-05179 and UBACYT/x053. We especially thank Daniel Grempel for very useful discussions.

## References

- [1] D. S. Fisher, Phys. Rev. Lett. **69**, 534 (1992); Phys. Rev. B **51**, 6411 (1995). Physica A **263**, 222 (1999).
- [2] M. Vojta, cond-mat/0412208 to appear in Phil. Mag.
- [3] P. Werner, K. Voelker, M. Troyer and S. Chakravarty, *Phase diagram and critical exponents of a dissipative Ising spin chain in a transverse magnetic field*, cond-mat/0402224. P. Werner, M. Troyer and S. Sachdev, *Quantum spin chains with site dissipation*, cond-mat/0412529.
- [4] S. Pankov, S. Florens, A. Georges, G. Kotliar and S. Sachdev, Phys. Rev. B **69**, 054426 (2004).
- [5] B. M. McCoy and T. T. Wu, Phys. Rev. **176**, 631 (1968), *ibid* **188**, 982 (1969).
- [6] S. Sachdev, *Quantum phase transitions*, (Cambridge University Press, Cambridge 1999).

- [7] A. Leggett, S. Chakravarty, A. Dorsey, M. Fisher, A. Garg and W. Zwerger, *Rev. Mod. Phys.*, **59**, 1 (1987). A. Caldeira and A. Leggett, *Phys. Rev. Lett.* **46**, 211 A. Caldeira and A. Leggett, *Ann Phys.* **149**, 374 (1983).
- [8] L. F. Cugliandolo, D. R. Grempel, G. Lozano, H. Lozza, C. A. da Silva Santos, *Phys. Rev. B* **66**, 014444 (2002).
- [9] L. F. Cugliandolo, D. R. Grempel, G. Lozano and H. Lozza, *Phys. Rev. B* **70**, 024422 (2004).
- [10] F. Iglói and H. Rieger, *Phys. Rev. B* **57**, 11404 (1998) F. Igloi, R. Juhasz, H. Rieger, *Phys. Rev. B* **59**, 11308 (1999). H. Rieger and F. Iglói, *Phys. Rev. Lett.* **83**, 3741 (1999). F. Igloi, R. Juhasz, P. Lajkó, *Phys. Rev. Lett.* **86**, 1343 (2001). D. Karevski, Y-C. Lin, H. Rieger, N. Kawashima, F. Iglói, cond-mat/0009144 F. Iglói, *Phys. Rev. B* **65**, 064416 (2002).
- [11] C. Monthus, *Phys. Rev. B* **69**, 054431 (2004).
- [12] H. Rieger and A. P. Young, *Phys. Rev. Lett.* **72**, 4141 (1994). *Phys. Rev. B* **54**, 3328 (1996).
- [13] M. Guo, R. Bhatt and D. Huse, *Phys. Rev. Lett.* **72**, 4137 (1994). *Phys. Rev. B* **54**, 3336 (1996).
- [14] A. P. Young and H. Rieger, *Phys. Rev. B* **53**, 8486 (1996). A. P. Young, *Phys. Rev. B* **56**, 11691-11700 (1997) D. S. Fisher and A. P. Young, *Phys. Rev. B* **58**, 9131 (1998).
- [15] C. Pich, A. P. Young, H. Rieger and N. Kawashima, *Phys. Rev. Lett.* **81**, 5916 (1998).
- [16] O. Motrunich, S.-C. Mau, D. A. Huse, and D. S. Fisher *Phys. Rev. B* **61**, 1160 (2000). O. Motrunich, K. Damle, and D. A. Huse *Phys. Rev. B* **63**, 224204 (2001).
- [17] N. Kawashima and H. Rieger, Recent progress in spin glasses, in *Frustrated spin systems*, H. T. Diep ed. (World Scientific, 2004).
- [18] A. H. Castro-Neto and B. A. Jones, *Phys. Rev. B* **62**, 14975 (2000). E. Novais *et al*, *Phys. Rev. Lett.* **88**, 217201 (2002), *Phys. Rev. B* **66**, 174409 (2002).
- [19] A. J. Millis, D. Morr and J. Schmalian, *Phys. Rev. Lett.* **87**, 167202 (2001), *Phys. Rev. B* **66**, 174433 (2002).

- [20] U. Weiss in Series Modern Condensed Matter Physics (World Scientific, Singapore, 1993) R. P. Feynman and Vernon, Jr. Ann. Phys. (NY) **24**, 118
- [21] U. Wolff, Phys. Rev. Lett. **62**, 361 (1989).
- [22] E. Luijten and H. W. K. Blote, Int. J. Mod. Phys. C **6**, 359 (1995).
- [23] A. M. Ferrenberg and R. H. Swendsen, Phys. Rev. Lett. **61**, 2635 (1988).
- [24] A. Crisanti and H. Rieger, J. Stat. Phys. **77**, 1087 (1994).
- [25] “The Monte Carlo Method in Condensed Matter Physics” edited by K. Binder, 2nd ed., (Topics in Applied Physics, Vol. 71), Springer-Verlag.
- [26] L. Onsager, Phys. Rev. **65**, 117 (1944).
- [27] When  $\alpha = 0$ ,  $B$  can be factorized in the effective  $2d$  classical action (6) as an inverse effective “temperature” showing close correspondance to the McCoy-Wu random Ising model [5]. Thus, in the McCoy-Wu model with uniform distribution of exchanges, the critical temperature,  $T_c$ , satisfies  $2/T_c + [\ln \tanh(J_i/T_c)] = 0$ . Then,  $B = 1/T_c = 0.70$  and through Eq. (7) we obtain  $\Delta\tau_c\Gamma_c = 0.25$ . In particular, for  $J_i = 1$  we recover the Onsager’s result with  $B = 1/T_c = 0.44$  and through Eq. (7) we obtain  $\Delta\tau_c\Gamma_c = 0.44$ .
- [28] We computed the global linear susceptibility shown in Sect. 4.1.2 using the expression in the right-hand-side of Eq. (14) and taking the magnetization with an absolute value in order to take into account the ergodicity breaking in the ferromagnetic phase [29]. This introduces a systematic shift in the peak of the susceptibility due to the fact that  $\langle m_i \rangle$  is not strictly zero on paramagnetic side, as it should.
- [29] D. P. Landau, Phys. Rev. B **13**, 2997 (1976).
- [30] Indeed, the susceptibility of the dissipative single quantum Ising spin for finite  $N_\tau$  also has a peak at a finite value of  $\Delta\tau\Gamma$  that moves extremely slowly towards smaller values when  $N_\tau$  increases. However, the values of  $N_\tau$  that one can easily reach numerically are not sufficient to safely extrapolate to zero. Another reason for this defect is that the way in which we compute  $\chi$  (explained in [28]) overestimates its value in the paramagnetic phase.

- [31] Since we are here interested in the paramagnetic phase only we computed the local linear susceptibility shown in Sect. 4.2.2 using  $\chi_i = N_\tau^{-1} \langle m_i^2 \rangle$  (and assuming  $\langle m_i \rangle = 0$ ).
- [32] A. Aharony, R. J. Birgeneau, A. Coniglio, M. A. Kastner, and H. E. Stanley, Phys. Rev. Lett. **60**, 1330 (1988). W. Wu, D. Bitko, T. F. Rosenbaum and G. Aeppli, Phys. Rev. Lett. **71** 1919 (1993). F. C. Chou, N. R. Belk, M. A. Kastner, R. J. Birgeneau, and A. Aharony Phys. Rev. Lett. **75**, 2204 (1995).
- [33] T. Senthil, A. Vishwanath, L. Balents, S. Sachdev, and M. P. A. Fisher, Science **303**, 1490 (2004).